AGU PUBLICATIONS

JGR

Journal of Geophysical Research: Biogeosciences

RESEARCH ARTICLE

10.1002/2013JG002591

**Key Points:**
- Tropical land carbon loss is a key uncertainty in climate change projections
- $CO_2$ interannual variability is linearly related to tropical carbon loss in CMIP5
- Observed variability in $CO_2$ constrains projections of future carbon losses

**Correspondence to:**
S. Wenzel,
Sabrina.Wenzel@dlr.de

**Citation:**
Wenzel, S., P. M. Cox, V. Eyring, and P. Friedlingstein (2014), Emergent constraints on climate-carbon cycle feedbacks in the CMIP5 Earth system models, *J. Geophys. Res. Biogeosci.*, *119*, 794–807, doi:10.1002/2013JG002591.

Received 6 DEC 2013
Accepted 4 APR 2014
Accepted article online 23 APR 2014
Published online 12 MAY 2014

# Emergent constraints on climate-carbon cycle feedbacks in the CMIP5 Earth system models

**Sabrina Wenzel[1], Peter M. Cox[2], Veronika Eyring[1], and Pierre Friedlingstein[2]**

[1]Deutsches Zentrum für Luft- und Raumfahrt, Institut für Physik der Atmosphäre, Oberpfaffenhofen, Germany, [2]College of Engineering, Mathematics and Physical Sciences, University of Exeter, Devon, UK

**Abstract** An emergent linear relationship between the long-term sensitivity of tropical land carbon storage to climate warming ($\gamma_{LT}$) and the short-term sensitivity of atmospheric carbon dioxide ($CO_2$) to interannual temperature variability ($\gamma_{IAV}$) has previously been identified by Cox et al. (2013) across an ensemble of Earth system models (ESMs) participating in the Coupled Climate-Carbon Cycle Model Intercomparison Project ($C^4$MIP). Here we examine whether such a constraint also holds for a new set of eight ESMs participating in Phase 5 of the Coupled Model Intercomparison Project. A wide spread in tropical land carbon storage is found for the quadrupling of atmospheric $CO_2$, which is of the order of $252 \pm 112$ GtC when carbon-climate feedbacks are enabled. Correspondingly, the spread in $\gamma_{LT}$ is wide ($-49 \pm 40$ GtC/K) and thus remains one of the key uncertainties in climate projections. A tight correlation is found between the long-term sensitivity of tropical land carbon and the short-term sensitivity of atmospheric $CO_2$ ($\gamma_{LT}$ versus $\gamma_{IAV}$), which enables the projections to be constrained with observations. The observed short-term sensitivity of $CO_2$ ($-4.4 \pm 0.9$ GtC/yr/K) sharpens the range of $\gamma_{LT}$ to $-44 \pm 14$ GtC/K, which overlaps with the probability density function derived from the $C^4$MIP models ($-53 \pm 17$ GtC/K) by Cox et al. (2013), even though the lines relating $\gamma_{LT}$ and $\gamma_{IAV}$ differ in the two cases. Emergent constraints of this type provide a means to focus ESM evaluation against observations on the metrics most relevant to projections of future climate change.

## 1. Introduction

In most climate-carbon cycle projections, climate warming reduces the efficiency of anthropogenic carbon dioxide ($CO_2$) absorption by the land and ocean [*Cox et al.*, 2000; *Friedlingstein et al.*, 2001, 2006]. As a result, more emitted carbon stays in the atmosphere leading to additional warming, representing a positive climate-carbon cycle feedback [*Friedlingstein et al.*, 2001, 2003].

The long-term sensitivity of land carbon storage to future climate warming ($\gamma_L$) can be quantified in terms of carbon loss per unit temperature change [*Friedlingstein et al.*, 2003], usually given in units of GtC/K. The differences in $\gamma_L$ simulated by the models remain a key uncertainty in climate projections of the 21st century [*Friedlingstein et al.*, 2006; *Booth et al.*, 2012]. However, $\gamma_L$ cannot be directly evaluated with observations, not only because the observational record is not yet long enough but also because $\gamma_L$ relates to a theoretical reference state in the absence of climate change, which is obviously not observable. The tropics make a dominant contribution to uncertainties in $\gamma_L$ [*Raddatz et al.*, 2007; *Huntingford et al.*, 2013]. Uncertainties in future projections of tropical rainfall, and in the response of ecosystems to these, are central to the overall uncertainty in the response of the land carbon cycle to climate change [*Jupp et al.*, 2010; *Rammig et al.*, 2010; *Huntingford et al.*, 2013].

In a recent study, *Cox et al.* [2013] found a correlation between the long-term sensitivity of tropical land carbon storage to climate warming ($\gamma_{LT}$) and the short-term sensitivity of atmospheric carbon dioxide ($CO_2$) to temperature variability on interannual time scales ($\gamma_{IAV}$). A correlation between the long-term and the short-term sensitivities can be expected if the processes that play for the long-term response are also driving the short-term fluctuations, i.e., if processes occurring on long time scales (such as vegetation dynamic) are not dominant. This is potentially the case here as both the short- and long-term responses of the tropical land to climate are predominantly driven by changes in the balance between the gross carbon fluxes, photosynthesis, and ecosystem respiration. Responses of the carbon cycle to climate anomalies are mirrored in the interannual variability (IAV) of the $CO_2$ growth rate [*Keeling et al.*, 1989, 1995; *Francey et al.*, 1995]. This relationship is especially valid in the tropics, where strong variability caused by El Niño gives a spatially coherent pattern of warmer and colder years [*Bousquet*, 2000].

**Table 1.** CMIP5 Models

| | Model | Institute | Atmospheric Resolution | Oceanic Resolution | Main Reference |
|---|---|---|---|---|---|
| A | CanESM2 | Canadian Center for Climate Modeling and Analysis, BC, Canada | T63, L35 | 256 × 192, L40 | *Arora et al.* [2011] |
| B | CESM1-BGC | National Center for Atmospheric Research Boulder, CO, USA | 0.9° × 1.25° gx1v6, L53 | 0.9° × 1.25° gx1v6, L53 | *Gent et al.* [2011] |
| C | GFDL-ESM2M | Geophysical Fluid Dynamics Laboratory, United States | M54, L24 | 360 × 200, L50 | *Dunne et al.* [2012] |
| D | HadGEM-ES | Met Office Hadley Center, Exeter, Devon, UK | N96, L38 | 1.0°–0.3° × 1.0°, L40 | *Collins et al.* [2011] |
| E | IPSL-CM5A-R | Institut Pierre Simon Laplace, Paris, France | 96 × 95, L39 | 2 × 2, L31 | *Dufresne et al.* [2013] |
| F | MIROC-ESM | Japan Agency for Marine-Earth Science and Technology, Japan; Atmosphere and Ocean Research Institute, Japan | T63, L80 | 256 × 192, L44 | *Watanabe et al.* [2011] |
| G | MPI-ESM-LR | Max Planck Institute for Meteorology, Hamburg, Germany | T63, L47 | GR15, L40 | *Giorgetta et al.* [2013] |
| H | NorESM1-ME | Norwegian Climate Center, Norway | f19, L26 | gx1v6, L53 | *Iversen et al.* [2012] |

The variability of tropical temperature and atmospheric $CO_2$ concentrations are both observable quantities, and therefore, $\gamma_{IAV}$ can be directly inferred from observations. A strong correlation between $\gamma_{IAV}$ and $\gamma_{LT}$ therefore provides an *Emergent Constraint* on the long-term sensitivity of land carbon storage to climate change. More generally, emergent constraints are relationships across an ensemble of models, between some aspect of the Earth system sensitivity and an observable trend or variation in the current climate [*Flato et al.*, 2013]. This is a relatively new area of research with some promising examples already studied in the literature, for example, constraints on the snow-albedo feedback [*Hall and Qu*, 2006; *Qu and Hall*, 2013], on Antarctic total column ozone projections [*Karpechko et al.*, 2013], on climate sensitivity based on variations in midtropospheric relative humidity and their impact on clouds [*Fasullo and Trenberth*, 2012], and on the sensitivity of tropical precipitation extremes to climate change [*O'Gorman*, 2012].

In this study, we begin to develop the theoretical basis for describing the emergent constraint reported by *Cox et al.* [2013]. We also extend that analysis by considering the more recent ensemble of Phase 5 of the Coupled Model Intercomparison Project (CMIP5) Earth system models (ESMs), including models with an interactive land nitrogen cycle which have the potential to change the correlation between $\gamma_{IAV}$ and $\gamma_{LT}$. In addition, we use land and ocean net $CO_2$ fluxes from the Global Carbon Project (GCP) to develop the observational constraint on $\gamma_{IAV}$, rather than the global atmospheric $CO_2$ concentration as in *Cox et al.* [2013]. This allows the approach to be applied to model runs with prescribed $CO_2$ concentrations and those with interactive atmospheric $CO_2$, and is more directly comparable to the carbon fluxes anomalies simulated in the ESMs. The sensitivity of $CO_2$ to tropical temperature IAV is calculated from two kinds of CMIP5 simulations: historical simulations driven by $CO_2$ emissions and standard simulations with a prescribed 1% per year increase in $CO_2$ concentration. We cross-check our results with models from the previous Coupled Climate-Carbon Cycle Model Intercomparison Project ($C^4$MIP), as used in the study of *Cox et al.* [2013], but using the new methodology presented here.

This paper is organized as follows: Section 2 describes the models and simulations used in this study. Section 3 provides an overview of the observations that are used to evaluate the models and to constrain the projections. The theoretical basis and the methodology for an emergent constraint are presented in section 4. In section 5, the results are presented and discussed, and section 6 closes with a summary.

## 2. Models and Model Simulations

In this study, we analyze the carbon cycle feedback constraints from eight ESMs participating in the CMIP5 project. CMIP5 supported the climate model projections presented in the Intergovernmental Panel on Climate Change Fifth Assessment Report and includes a large number of different experimental designs [*Taylor et al.*, 2012]. The model data are available to the research community via the Earth System Grid Federation (ESGF). The models that are included in this study are listed in Table 1 together with their atmospheric and oceanic grids, and an appropriate reference.

**Table 2.** Overview of the Simulation Experiments in This Study

| | Experiment | Coupling of Carbon Cycle | Available Period | Temporal Resolution | Forcing |
|---|---|---|---|---|---|
| 1 | *Historical* | Fully coupled | 1850–2005 | monthly | greenhouse gases, anthropogenic and volcanic climate forcing, land use change, solar forcing, and aerosols |
| 2 | *1%COU2* | Fully coupled | 0–140 | monthly | 1%/yr $CO_2$ increase |
| 3 | *1%BGC* | uncoupled | 0–140 | monthly | 1%/yr $CO_2$ increase |

For this study, model outputs from three simulations were analyzed and are listed in Table 1. The *esmHistorical* (hereafter referred to as "Historical") experiment is a fully coupled simulation from 1850 to 2005 with historical anthropogenic emissions of $CO_2$, atmospheric concentrations being calculated interactively by the ESM as the balance between anthropogenic emissions and uptakes by the land and ocean [*Taylor et al.*, 2012]. The *1pctCO2* (hereafter referred to as "1%COU") simulation is a standard idealized experiment forced with a 1%/yr increase of atmospheric $CO_2$ concentration up to $4 \times CO_2$, starting from the preindustrial value for 1850 of ~285 ppmv. The third simulation also considers a 1%/yr increase of $CO_2$, but in which the carbon cycle is not affected by any climate change (*esmFixClim1*, hereafter referred to as "1%BGC", the biogeochemically coupled simulation). In this latter simulation (termed as the "uncoupled run" by *Friedlingstein et al.* [2003, 2006]), the radiation code of the ESM sees the control preindustrial $CO_2$ concentration (so that there is no associated climate change), but the carbon cycle otherwise sees a 1%/yr increase in atmospheric $CO_2$. As opposed to the Historical simulation that account for all known forcings (greenhouse gases, aerosols, land use change, and volcanoes), the two 1%/yr simulations are only forced with the $CO_2$ increase; all other forcings are held at their preindustrial levels.

From the CMIP5 models that were available on the ESGF by summer 2013, we selected those that provide both land and ocean carbon fluxes and storage for all three experiments. For details of these models, see Table 1. Table 3 lists details of the land and ocean carbon representation for each model. For comparison, we also analyzed six models from the Coupled Climate-Carbon Cycle Model Intercomparison Project ($C^4$MIP) [*Friedlingstein et al.*, 2006]. For $C^4$MIP, the coupled and uncoupled simulations were forced by anthropogenic $CO_2$ emissions for the historical period, followed by anthropogenic emissions from the Special Report on Emissions Scenarios A2 scenario [*Nakicenovic et al.*, 2000].

## 3. Observations for Model Evaluation

To calculate the observational estimate of $\gamma_{IAV}$, we used land and ocean carbon fluxes from the Global Carbon Project (GCP, http://www.tyndall.ac.uk/global-carbon-budget-2010). For each year since 1959, GCP provides a global $CO_2$ budget, reporting the fossil fuel and the land use change emission data, the observed atmospheric $CO_2$ growth rate, an estimate of the ocean carbon uptake from four ocean biogeochemical models constrained by observed oceanic uptake data, and the land carbon uptake as the residual of atmospheric $CO_2$ and ocean carbon fluxes [*Le Quéré et al.*, 2013].

Annual mean temperatures from the NOAA–National Climate Data Center (NCDC, http://www.esrl.noaa.gov/psd/data/gridded/data.noaamergedtemp.html) were used to estimate the interannual variability in the

**Table 3.** Overview of Land and Ocean Carbon Modules in CMIP5 Model

| | Model | Land Models | References for Land Model | Ocean Models | References for Ocean Models |
|---|---|---|---|---|---|
| A | CanESM2 | CLASS2.7 and CTEM1 | *Verseghy et al.* [1993] and *Arora et al.* [2011] | CMOC | *Zahariev et al.* [2008] |
| B | CESM1-BGC | CLM4 | *Lawrence et al.* [2011] | BEC | |
| C | GFDL-ESM2M | LM3 | *Dunne et al.* [2012] | MOM4 | *Griffies et al.* [2004] |
| D | HadGEM-ES | JULES and TRIFFID | *Cox* [2001] and *Clark et al.* [2011] | Diat-HadOCC | *Collins et al.* [2011] |
| E | IPSL-CM5A-R | ORCHIDEE | *Krinner* [2005] | PISCES | *Aumont* [2003] |
| F | MIROC-ESM | MATSIRO and SEIB-DGVM | *Sato et al.* [2007] | COCO | *Watanabe et al.* [2011] |
| G | MPI-ESM-LR | JSBACH | *Knorr* [2000] | HAMOCC5 | *Assmann et al.* [2010] |
| H | NorESM1-ME | CLM4 | *Lawrence et al.* [2011] | HAMOCC5 | *Assmann et al.* [2010] |

tropics (30°S–30°N). This data set covers the period from 1880 to the present day at a monthly resolution [*Smith et al.*, 2008].

## 4. Theoretical Basis and Methodology

### 4.1. Theoretical Basis for the Emergent Constraint

The change of land carbon over time, $\frac{\partial \Delta C_L}{\partial t}$, can be defined as the net carbon flux from land to atmosphere (Net Biome Productivity—NBP) that depends on the temperature ($T$), the atmospheric $CO_2$ concentration ($C_a$), and the stored carbon on land ($C_L$):

$$\frac{\partial \Delta C_L}{\partial t} = \mathrm{NBP}\ (T, C_a, C_L) \tag{1}$$

As in previous studies [*Friedlingstein et al.*, 2003, 2006], we have implicitly assumed here that the impacts of other environmental changes, such as changes in rainfall, scale approximately linearly with the magnitude of the warming. This assumption is broadly consistent with the success of pattern scaling [*Huntingford and Cox*, 2000]. Linearizing equation (1) by Taylor expanding about an initial equilibrium state leads to the following:

$$\frac{\partial \Delta C_L}{\partial t} = a\ \Delta \mathrm{T} + b\ \Delta C_a + c\ \Delta C_L \tag{2}$$

where $a$, $b$, and $c$ denote $\frac{\partial \mathrm{NBP}}{\partial T}; \frac{\partial \mathrm{NBP}}{\partial C_a}; \frac{\partial \mathrm{NBP}}{\partial C_L}$ and $\Delta C_L, \Delta C_a$ and $\Delta T$ are changes relative to the initial state in land carbon uptake, $CO_2$, and temperature, respectively. Rewriting equation (2) and defining the constants $a$, $b$, and $c$ for consistency with *Friedlingstein et al.* [2006] gives the following:

$$\tau\ \frac{\partial \Delta C_L}{\partial t} + \Delta C_L = \ \gamma_L \Delta T + \beta_L\ \Delta C_a \tag{3}$$

with

$$-\frac{a}{c} = \gamma_L : \text{land carbon storage sensitivity to climate change} \tag{4.1}$$

$$-\frac{b}{c} = \beta_L : \text{land carbon sensitivity to direct } CO_2 \text{effects} \tag{4.2}$$

$$-\frac{1}{c} = \tau : \text{time scale of the carbon system} \tag{4.3}$$

Equation (3) is as proposed by *Friedlingstein et al.* [2003, 2006], except for the first term on the left-hand side. It is, however, vital to include this "inertial" term as it enables us to relate short-term variability to long-term sensitivity. To show this, we consider the following two limits:

1. On long (centennial) time scales, the interannual variability in the carbon cycle is much smaller than the long-term changes which means that $\tau \frac{\partial \Delta C_L}{\partial t} \ll C_L$ and the first term in equation (3) is negligible. The resulting equation is the one published by *Friedlingstein et al.* [2003, 2006] and describes the long-term change of land carbon uptake depending on the change in temperature and atmospheric $CO_2$:

   $$\Delta C_L = \ \gamma_L \Delta \mathrm{T} + \beta_L \Delta C_a \tag{5}$$

   From equation (5), $\gamma_L$, or its regional equivalents such as $\gamma_{\mathrm{LT}}$ for the tropics, can be calculated as in previous studies [*Friedlingstein et al.*, 2003, 2006].
2. On short (interannual) time scales, changes in the long-term trend will be close to zero ($\Delta C_L \sim 0, \Delta C_a = 0$) and the second term in equation (3) is now negligible. This limit gives a relationship between the long-term sensitivity of land carbon storage to climate change $\gamma_L$ and the short-term sensitivity of the net atmosphere to land carbon flux to interannual temperature variations, $\gamma_{\mathrm{NBP}} = \frac{\partial \Delta C_L}{\partial t} / \Delta T$:

   $$\gamma_{\mathrm{NBP}} = \ {}^{\gamma_L}\big/_{\tau} \tag{6}$$

   Here as elsewhere in this paper, the subscript "L" represents "Land" and the subscript "NBP" denotes the "Net Biome Productivity". Equation (6) is in the spirit of the Fluctuation-Dissipation Theorem [*Leith*, 1975; *Bell*, 1980] as it is a relationship between the equilibrium sensitivity of the system to external forcing, and the fluctuations in the unperturbed system.

However, equation (6) does not in itself imply an observational constraint on $\gamma_L$, for two reasons. First, in general, the NBP of a region is poorly known so that $\gamma_{NBP}$ is not well constrained by observations. Second, the time scale $\tau$ is not known a priori. We follow *Cox et al.* [2013] to overcome these problems. By focusing specifically on tropical land (30°N–30°S), it is possible to get an estimate of $\gamma_{NBP}$ based on the interannual variability in atmospheric $CO_2$, making use of the strong evidence that interannual variability in $CO_2$ is dominated by interannual variability in the NBP of tropical land [*Denman et al.*, 2007; *Schneising et al.*, 2014]. This implies assuming $\gamma_{NBP\sim}\ \gamma_{IAV=} -\frac{\partial \Delta CO_2}{\partial t}/\Delta T$, where here $\Delta CO_2$ is the interannual variability in $CO_2$, and $\Delta T$ is the interannual variability in temperature. Under this assumption, equation (6) becomes

$$\gamma_{IAV\sim}{}^{\gamma_{LT}}\Big/_{\tau} \tag{7}$$

where the subscript "LT" now applies specifically to land in the tropics. Given an estimate of $\tau$, equation (7) provides a constraint on the long-term sensitivity from the observable $\gamma_{IAV}$.

The outstanding issue is therefore the estimation of $\tau$, which is the subject of ongoing research. The Fluctuation-Dissipation Theorem (FDT) indicates that $\tau$ could in principle be derived from the correlogram relating fluctuations in tropical temperature to fluctuations in atmospheric $CO_2$, by integrating across all lag periods between these two variables [*Bell*, 1980]. Unfortunately, the time series data available from observations are invariably too short for this pure FDT approach to provide a useful constraint [*Kirk-Davidoff*, 2009].

As an alternative, we could assume that tropical land carbon behaves approximately like a one-box store with a single turnover time. In this case, $\tau$ becomes the carbon turnover time, defined as the size of the store (i.e., the total vegetation plus soil carbon in the tropics) divided by the annual flux of carbon flowing through that store (i.e., the Net Primary Productivity in the tropics). Previous studies have shown that the turnover times for land carbon differ substantially across ESMs [*Anav et al.*, 2013], and we would therefore not expect a plot of $\gamma_{LT}$ against $\gamma_{IAV}$ to fit around a single straight line in the way that *Cox et al.* [2013] describe for the $C^4$MIP models.

In fact, equation (7) implies that the linear relationship between $\gamma_{LT}$ and $\gamma_{IAV}$ reported by *Cox et al.* [2013] in turn implies a near constant value of $\tau$ across the model ensemble. As the turnover time for tropical land carbon also differs for the $C^4$MIP models (although to a lesser degree than for the CMIP5 models), this strongly suggests that the $\tau$ value relating $\gamma_{LT}$ to $\gamma_{IAV}$ is not determined by the turnover rates of tropical land carbon, but instead by a time scale that is common to all of the $C^4$MIP model runs.

We suggest that the most likely candidate for such a time scale is related to the rate of climate change, which is largely determined by the common scenario of increases in $CO_2$ emissions prescribed in all of the $C^4$MIP models [*Friedlingstein et al.*, 2006]. Similarly, the CMIP5 simulations analyzed in this paper experience a common time scale associated with the prescribed 1% per year increase in atmospheric $CO_2$, which differs slightly from the scenario time scale of the $C^4$MIP models.

Our working hypothesis is therefore that the CMIP5 models will also fit around a straight line in the $\gamma_{LT}$ and $\gamma_{IAV}$ space, but that this straight line may have a different gradient to that for the $C^4$MIP models, owing to the different scenarios prescribed in each of these intercomparison exercises. The analysis presented in the remainder of this paper allows this hypothesis to be tested and most importantly assesses whether the emergent constraint on $\gamma_{LT}$ as reported by *Cox et al.* [2013] is robust to changes in the ESM model generation and the prescribed climate change scenario.

### 4.2. Methodology

As in *Friedlingstein et al.* [2003, 2006], we apply equation (5) separately to the tropical land carbon in the coupled and uncoupled simulations:

$$\Delta C_{LT^c} = \gamma_{LT}\Delta T_{T^c} + \beta_{LT}\Delta C_{a^c} \tag{8.1}$$

$$\Delta C_{LT^u} = \gamma_{LT}\Delta T_{T^u} + \beta_{LT}\Delta C_{a^u} \tag{8.2}$$

where $\Delta T_T$ is the change in the average tropical near-surface temperature (over land and ocean between 30°N and 30°S), and the superscripts "c" and "u" denote the coupled and uncoupled simulations, respectively.

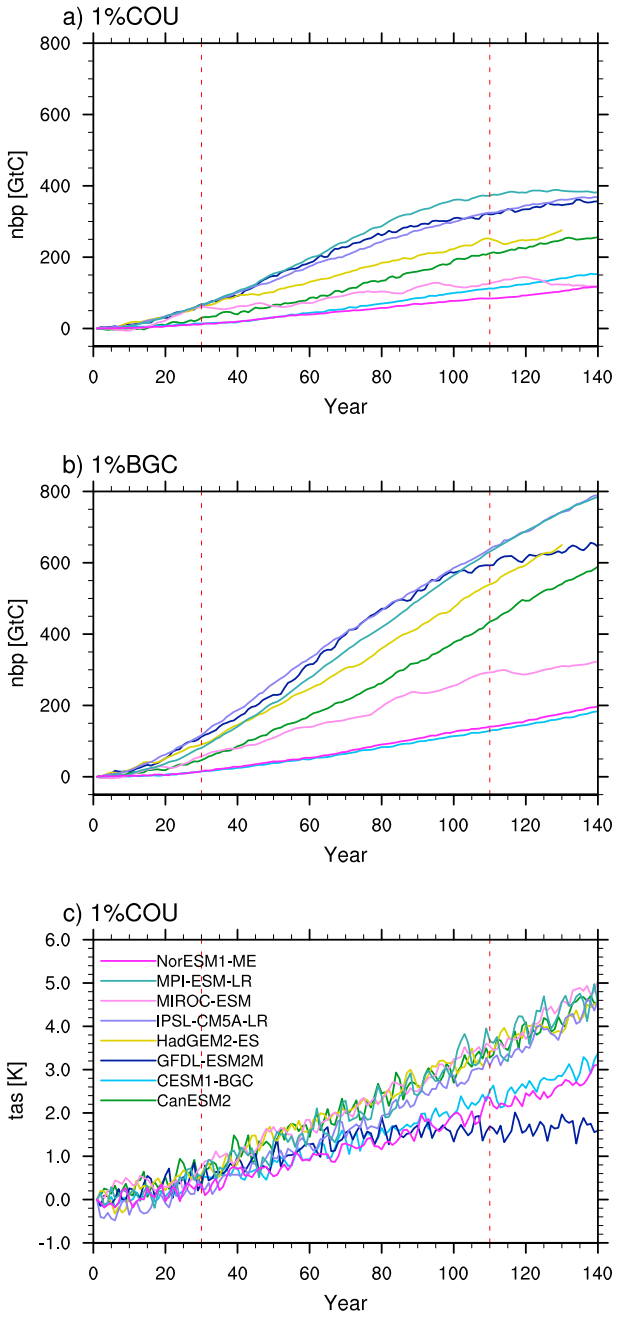


**Figure 1.** Quantities used to diagnose $\gamma_{LT}$. Cumulative tropical land carbon uptake for (a) the coupled simulation, (b) the uncoupled simulation, and (c) the projected tropical (30°N–30°S) mean near-surface air temperature (tas) change in the prescribed $CO_2$ coupled simulation (1%COU), for the CMIP5 models listed in Table 1. The simulations are forced by 1%/yr rise in $CO_2$ until quadrupling, except in the GDFL-ESM2M model, which prescribed a constant $CO_2$ after doubling. Vertical red lines show the interval over which $\gamma_{LT}$ was calculated.

In contrast to *Cox et al.* [2013], we use the coupled (1%COU) and uncoupled (1%BGC) 1%/yr simulations to estimate $\Delta C_L$. As the $CO_2$ concentration is prescribed to be identical in the coupled and uncoupled runs, $\Delta C_a^c$ equals $\Delta C_a^u$. In addition, we follow *Friedlingstein et al.* [2003, 2006] in assuming $\Delta T_{T^c} \gg T_{T^u}$. Although there may be small temperature changes in the uncoupled simulations, for example, due to $CO_2$-induced changes in the distribution of vegetation, these are negligible compared to the temperature changes in the coupled simulations (1% to less than 5% depending on the ESM). Under these assumptions, the equations for the coupled and uncoupled changes can be subtracted to yield an expression for $\gamma_{LT}$ which depends on the difference between the tropical land carbon storage of the coupled (1%COU) and uncoupled (1%BGC) simulations, and the temperature change in the coupled simulation

$$\gamma_{LT} = \frac{\Delta C_{LT}^c - \Delta C_{LT}^u}{\Delta T_T^c} \quad (9)$$

The changes in these variables are computed for the tropical band (30°N–30°S) as the difference between year 110 and year 30 after the start of the simulation at 1850 $CO_2$ concentration levels.

In order to calculate the short-term fluctuation, land and ocean $CO_2$ annual fluxes and tropical annual mean temperature from the models and the observations are detrended using an 11 year running mean, as in *Cox et al.* [2013]. The gradient of the least squares linear regression between anomalies in the $CO_2$ growth rate and the tropical temperature defines $\gamma_{IAV}$. An advantage of calculating $\gamma_{IAV}$ from the annual mean land and ocean $CO_2$ fluxes is that the tropical temperature does not have to be aligned to the annual increment in $CO_2$ [*Jones and Cox*, 2005; *Cox et al.*, 2013], as both are already centered in time in the middle of each year.

To assess robustness, $\gamma_{IAV}$ is calculated from both the Historical and the 1%COU simulation. For the Historical simulation, we exclude data for 2 years following large volcanic eruptions (Mount Agung, 1963; El Chichon, 1982; and Mount Pinatubo, 1991), as *Cox et al.* [2013], and calculate $\gamma_{IAV}$ over the period 1960 to 2005 in both models and observations. In the 1%COU simulation, a reference period from 40 to 90 years after the start of the simulation in 1850 is chosen, thus representing a warmer climate than

**Table 4.** Overview of the Derived Sensitivities $\gamma_{LT}$ and $\gamma_{IAV}$, Listed for Each Model

| | Model | $\gamma_{LT}$ (GtC/K) [b] | $\gamma_{IAV}$ Historical (GtC/yr/K) [a,c] | $\gamma_{IAV}$ 1%COU (GtC/yr/K) [c] |
|---|---|---|---|---|
| A | CanESM2 | −74.3 | −7.4 ± 1.1 | −16.2 ± 1.2 |
| B | CESM1-BGC | −6.7 | 0.2 ± 1.1 | −3.5 ± 0.8 |
| C | GFDL-ESM2M | −116.4 | −12 ± 1.6 | −13.1 ± 2.1 |
| D | HadGEM-ES | −60.2 | −5.9 ± 0.7 | −7.9 ± 1.5 |
| E | IPSL-CM5A-LR | −22.9 | −3.7 ± 1 | −6.6 ± 1.6 |
| F | MIROC-ESM | −58.4 | −6.9 ± 1.7 | −10.7 ± 1.4 |
| G | MPI-ESM-LR | −78.3 | −0.5 ± 0.9 | −6.9 ± 0.6 |
| H | NorESM1-ME | −7.2 | −0.8 ± 0.9 | −2.9 ± 0.7 |
| I | OBS | - | −4.4 ± 0.9 | - |

[a]The uncertainty is given as the standard deviation.
[b]Calculated from equation (9), as the difference of cumulated land carbon flux between the coupled (1%COU) and uncoupled (1%BGC) simulation.
[c]Correlation between the global $CO_2$ IAV from land plus ocean carbon fluxes and tropical (30°N–30°S) temperature IAV.

today. We have tested the robustness of this choice by calculating $\gamma_{IAV}$ (and $\gamma_{LT}$ above) also for different periods, which yielded very similar results (not shown).

## 5. Results

### 5.1. Climate-Carbon Cycle Feedback Constraints in CMIP5 Models

In both experiments with prescribed $CO_2$ (i.e., 1%COU and 1%BGC), all models were forced by 1% increase of $CO_2$ until quadrupling, except the GFDL-ESM2M model simulation, which stopped increasing $CO_2$ at the time of $CO_2$ doubling (year 80) and kept the $CO_2$ concentration thereafter. The results for GFDL-ESM2M are therefore not comparable to the other models after year 80. The simulated tropical temperature change in the $CO_2$ prescribed coupled simulations (1%COU) shows significant differences among the models at the time of $CO_2$ quadrupling (year 140 in Figure 1c), ranging from around 3 to 5 K (excluding GFDL-ESM2M). CESM1-BGC and NorESM1-ME show a slower increase in tropical temperature than the other five models.

There is also a wide spread in the tropical land carbon storage among the CMIP5 models (Figure 1), which is of the order of 117–381 GtC for the coupled (1%COU, Figure 1a) and 182–788 GtC for the uncoupled (1%BGC, Figure 1b) simulations. Due to holding $CO_2$ at $2 \times CO_2$ after the time of concentration doubling (year 80), the evolution of tropical land carbon storage of GFDL-ESM2M flattens in both simulations after atmospheric $CO_2$ stabilization.

From the difference of coupled and uncoupled simulations, the climate-carbon cycle sensitivity $\gamma_{LT}$ can be quantified in terms of carbon loss per unit temperature increase. $\gamma_{LT}$ values for each model are listed in Table 4. Confirming the findings of previous studies [*Cox et al.*, 2000; *Friedlingstein et al.*, 2001, 2006; *Arora et al.*, 2013], all models show a negative $\gamma_{LT}$. However, there is a wide range of results in $\gamma_{LT}$, ranging from −6.7 GtC/K in CESM1-BGC to −116.4 GtC/K in GFDL-ESM2M.

It is interesting to note that CESM1-BGC and NorESM1-ME simulate the weakest climate change impact on tropical land carbon storage. The CLM4 land surface model, used in both of these ESMs (Table 3), includes an interactive nitrogen cycle. Therefore, in these models, warming not only leads to carbon loss from enhanced soil decomposition but also a counteracting carbon gain due to enhanced photosynthesis associated with increased soil nitrogen availability. The overall effect depends on the balance between these two effects but is always lower (less negative $\gamma_{LT}$) than in carbon-only models [*Thornton et al.*, 2007, 2009; *Zaehle et al.*, 2010].

The $\gamma_{IAV}$ is calculated over the period 1960–2005 for the historical simulations (Figures 2a, 2c, 2e, and 3) for consistency with the $CO_2$ observational data that we used, and over the period year 40 to year 90 from the 1%COU simulations (Figures 2b, 2d, 2f, and 4). The variability of both carbon fluxes and tropical temperature is found to vary widely across the ESMs (range in Figures 2–4), as does the strength of the correlation between $CO_2$ IAV and temperature IAV (linear regression in Figures 3 and 4). The $\gamma_{IAV}$ varies from zero (nonsignificant) for CESM1-BGC to −12 GtC/yr/K for GFDL-ESM2M, with a multimodel average of −4.6 GtC/yr/K.

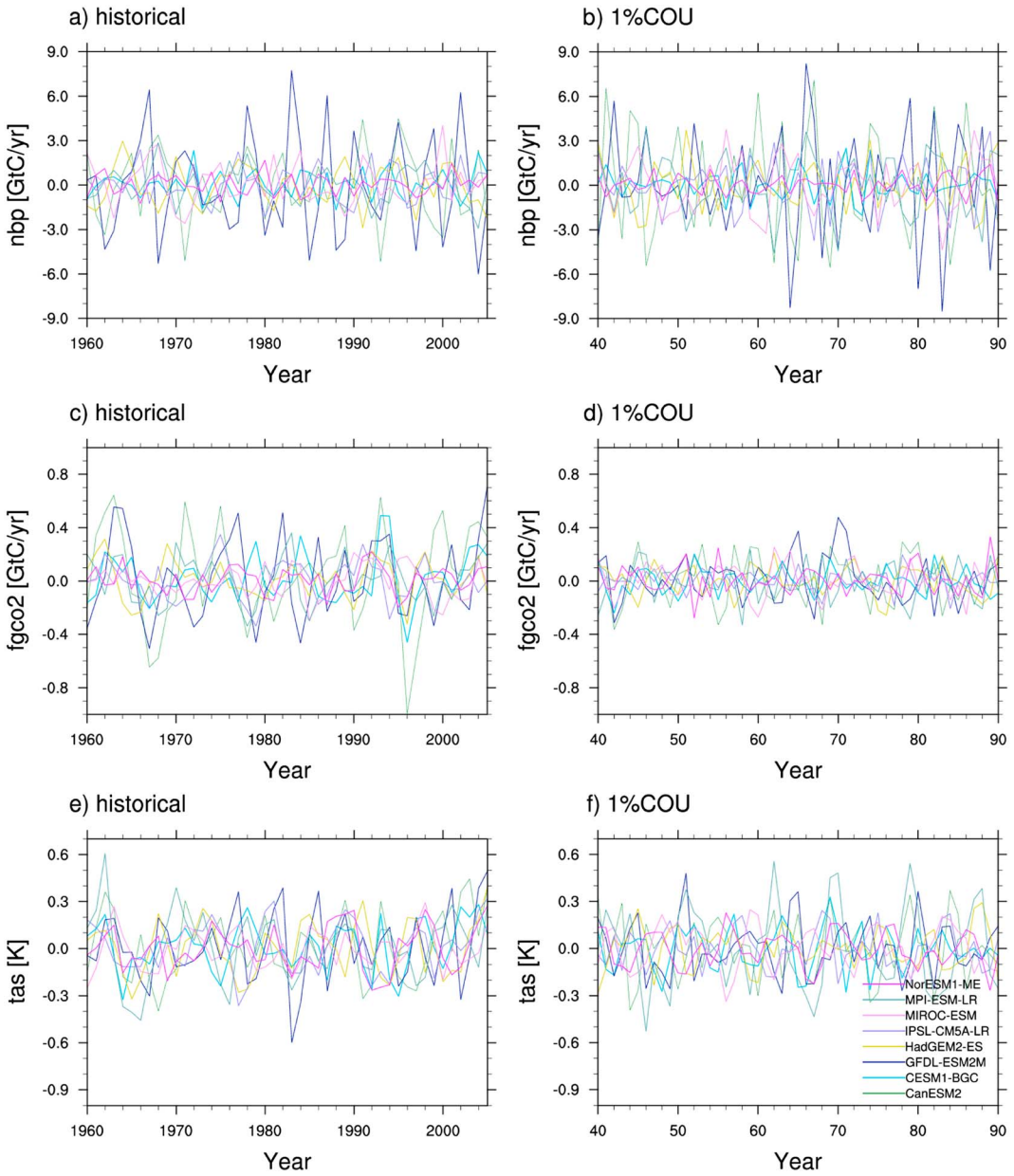


**Figure 2.** Quantities used to diagnose $\gamma_{IAV}$, each displayed in the applied period. Anomalies of the (a and b) global land carbon flux, (c and d) global ocean carbon flux, and (e and f) tropical near-surface temperature calculated from the Historical simulation in Figures 2a, 2c, and 2e and from the 1%COU simulation in Figures 2b, 2d, and 2f, for CMIP5 models listed in Table 1.

The observed $\gamma_{IAV}$, derived from the sum of the GCP land and ocean fluxes versus the IAV of tropical (30°S–30°N) temperature from NCDC data, yields a $\gamma_{IAV}$ of $-4.4 \pm 0.9$ GtC/yr/K with a correlation coefficient of $r = -0.60$ (Figure 3i). This compares with the value quoted by *Cox et al.* [2013] of $5.1 \pm 0.9$ GtC/yr/K, using a different method based on annual mean $CO_2$ concentrations rather than fluxes, and for a slightly longer period (1960–2010). GFDL-ESM2M and CanESM2 have the highest values of $\gamma_{IAV}$ of $-12$ GtC/yr/K and $-7.4$ GtC/yr/K, respectively (Figures 3a and 3c). CESM1-BGC and NorESM1-ME show the smallest $\gamma_{IAV}$, 0.2 GtC/yr/K and $-0.8$ GtC/yr/K (Figures 3b and 3h), which is much lower than the observations. These two models also show weak correlation between $CO_2$ IAV and temperature IAV ($r = 0.03$ and $r = -0.14$, respectively).

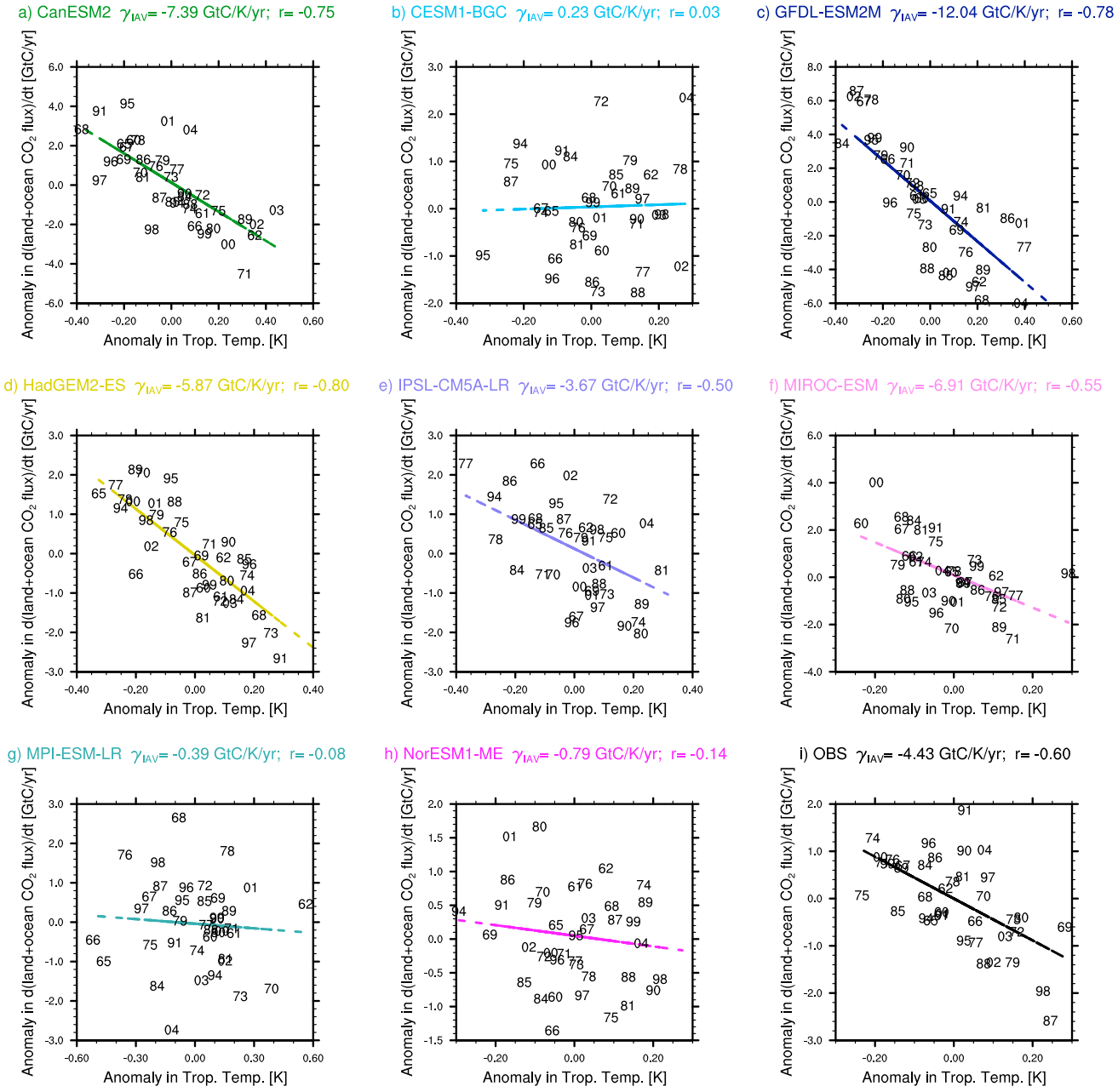


**Figure 3.** (a–i) Correlation between the IAV of the sum of the global land and ocean $CO_2$ fluxes and tropical temperature from Historical, shown for each model and the observations. Numbers indicate single years and colored lines are the best fit linear regression excluding the years after volcanic eruptions.

Plotting $\gamma_{LT}$ against $\gamma_{IAV}$ reveals the emergent constraint identified by *Cox et al.* [2013], and we do this for both the Historical simulations and the 1%COU simulations (Figure 5) to test for robustness. In both cases, there is evidence of a linear relationship between $\gamma_{LT}$ and $\gamma_{IAV}$, which holds for all the models apart from MPI-ESM-LR. This model shows a surprising net negative correlation between variations in soil respiration and temperature, most likely due to a strong suppression of soil respiration under reducing soil moisture, which overwhelms the usual increase in soil respiration with warming [*Ciais et al.*, 2005; *Reichstein et al.*, 2007; *Zaehle et al.*, 2010]. As a result, MPI-ESM-LR has unusually high soil carbon in dry regions, which is vulnerable to climate change (Figure 5a). It therefore seems that MPI-ESM-LR does not fit on the $\gamma_{IAV}$ $\gamma_{LT}$ correlation line (Figure 5a) as its short-term response is driven by different processes (the suppression of heterotrophic

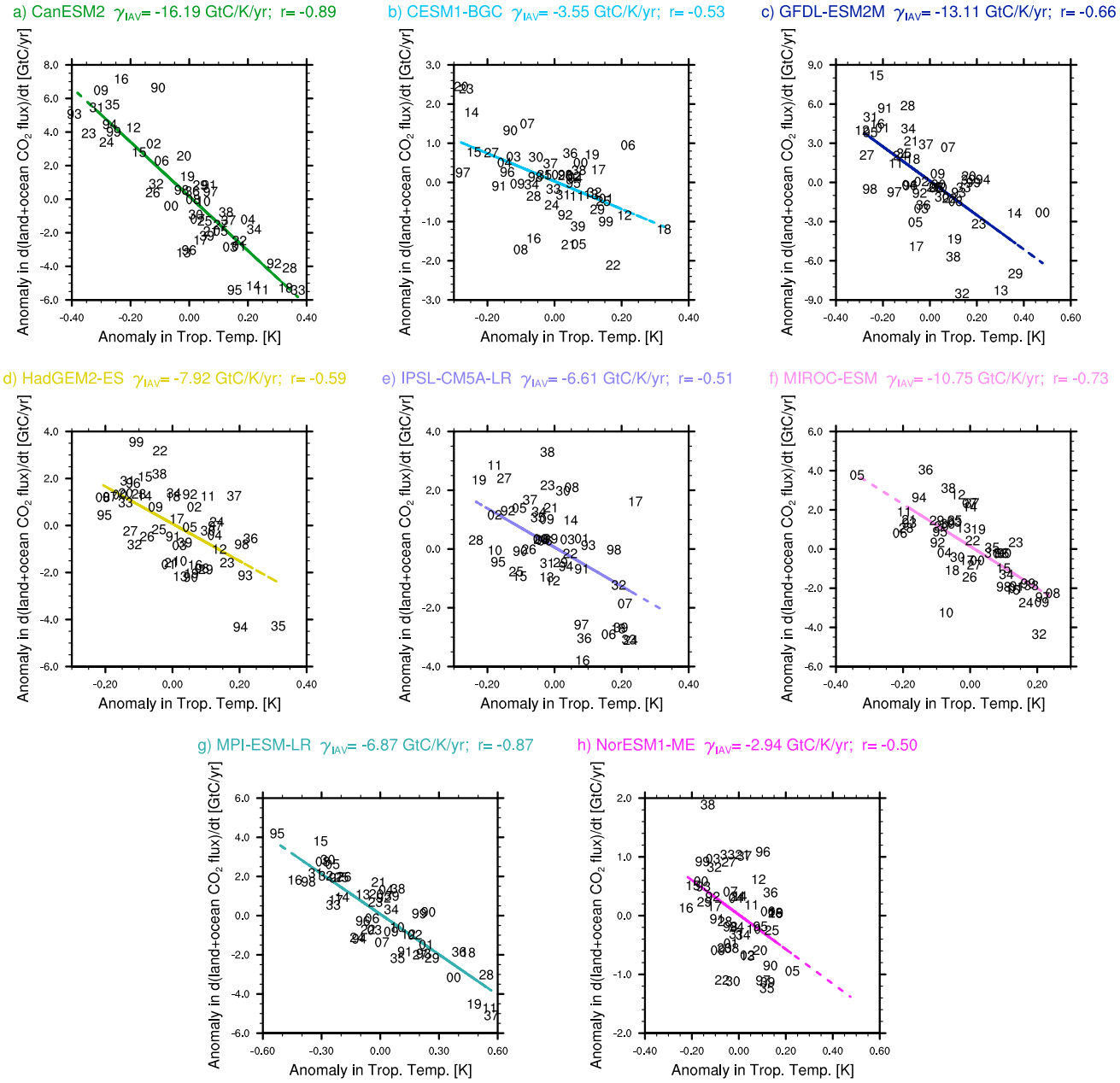


**Figure 4.** As for Figure 3, but using 1%COU simulations. Note that there is no observation panel here.

respiration by soil aridity) than the long-term response (decline in net primary productivity and hence in carbon storage). We have excluded MPI-ESM-LR when calculating the best fit linear regression.

Interestingly, although both CESM1-BGC and NorESM1-ME include nitrogen limitations [*Lawrence et al.*, 2011], these two models appear to fit the same line as the carbon-only models. This suggests that the inclusion of the nitrogen cycle does not change the relationship between the short- and long-term responses of tropical land carbon to climate, even though these models yield much lower values of $\gamma_{IAV}$ and $\gamma_{LT}$.

In the Historical experiment, the models can be constrained by the calculated observational estimate of $\gamma_{IAV} = -4.4 \pm 0.9$ GtC/yr/K. Without the observational constraint, all models would be equally likely to give the true $\gamma_{LT}$ in both experiments, which is shown as the dashed red lines in Figures 5b and 5d as a probability density function (PDF, calculated following *Cox et al.* [2013]). Using the observed $\gamma_{IAV}$ as constraint, a conditional PDF can be calculated. This is achieved by integrating over a contour PDF, which follows from

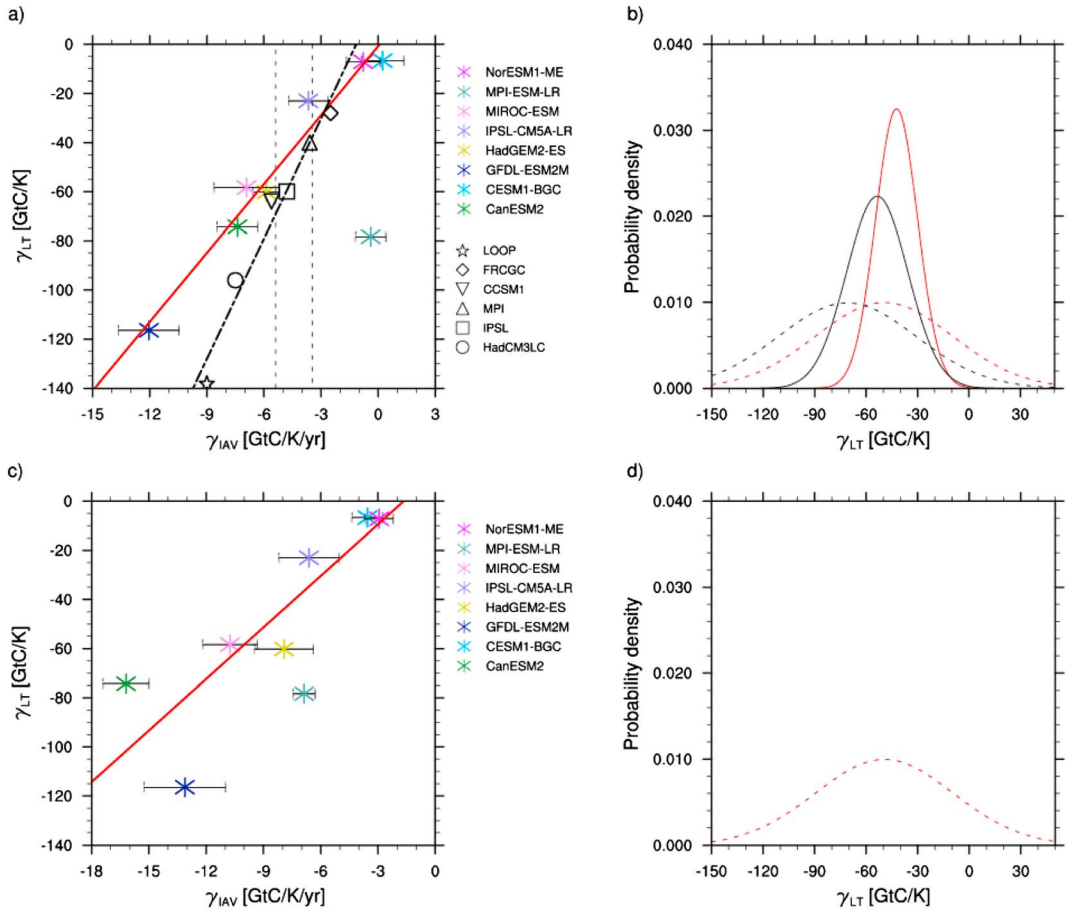


**Figure 5.** (a) The long-term sensitivity of tropical land carbon storage to climate warming ($\gamma_{LT}$) versus the short-term sensitivity of atmospheric $CO_2$ to interannual temperature variability ($\gamma_{IAV}$) for the CMIP5 and $C^4$MIP models. The red line shows the best fit line across the CMIP5 models using the Historical simulation. The vertical dashed lines show the range of the observed $\gamma_{IAV}$ according to Figure 3. (b) PDF for $\gamma_{LT}$. The solid line was derived after applying the IAV constraint to the models while the dashed line is the prior PDF derived purely from the models, before applying the IAV constraint. Red lines show PDFs for CMIP5 models and black lines and symbols are for $C^4$MIP models. (c and d) Same as Figures 5a and 5b but with $\gamma_{IAV}$ calculated from the 1%COU simulations.

multiplying the PDF of the observations and the PDF of the regression line. This conditional PDF gives a sharper peak with slightly less negative values and a much tighter range on the $\gamma_{LT}$. The conditional PDF gives $\gamma_{LT} = -44 \pm -14$ GtC/K, whereas the unconditional PDF gives $\gamma_{LT} = -49 \pm 40$ GtC/K for the CMIP5 models in the Historical experiment (Figure 5b).

### 5.2. Comparison With $C^4$MIP Models

To test for robustness, we compare our results to the findings of *Cox et al.* [2013] who derived a similar constraint from $C^4$MIP models (Figure 5a, black symbols). The correlation between $\gamma_{LT}$ and $\gamma_{IAV}$ across the $C^4$MIP ($r = 0.98$) models is as tight as for the CMIP5 models but the slope is slightly different. Most importantly, the best fit linear regression lines intercept close to the observational range and therefore give a similar emergent constraint on $\gamma_{LT}$. The calculated conditional PDF gives $-53 \pm -17$ GtC/K for the $C^4$MIP models as compared to $-44 \pm -14$ GtC/K for the CMIP5 ESMs.

## 6. Summary

An observation-based emergent constraint for the long-term sensitivity of land carbon storage to future climate warming ($\gamma_{LT}$) has been derived from an ensemble of eight Earth system models (ESMs) participating in the Fifth Phase of the Coupled Model Intercomparison Project (CMIP5). The $\gamma_{LT}$ cannot be directly

derived from observations, yet it remains a key uncertainty in climate projections of the 21st century. A previous study by *Cox et al.* [2013] based on models participating in the Coupled Climate-Carbon Cycle Model Intercomparison Project ($C^4$MIP) has already shown that the long-term climate sensitivity $\gamma_{LT}$ is highly correlated with the short-term sensitivity of atmospheric carbon dioxide ($CO_2$) to temperature variability ($\gamma_{IAV}$).

In this paper, a mathematical formulation for the emergent constraint between $\gamma_{LT}$ and $\gamma_{IAV}$ has been developed, which shows that the long- and short-term sensitivities are approximately related to each other through a time scale $\tau$.

To test whether the emergent constraint holds in an ensemble different than $C^4$MIP, a subset of eight ESMs was selected from the larger CMIP5 ensemble because the necessary output (surface downward $CO_2$ flux, carbon mass flux out of the atmosphere due to net biosphere production on land, and near-surface air temperature) was provided from two simulations with fully coupled carbon cycle (Historical and 1%COU) and one where the carbon cycles was insensitive to climate change (1%BGC). The first experiment is a historical simulation where the carbon cycle is fully coupled and $CO_2$ emissions calculated interactively (Historical). In the second simulation, $CO_2$ is prescribed with a 1%/yr increase until quadrupling, starting at a preindustrial value of ~285 ppmv (1%COU), except in one model (GFDL-ESM2M) where the forcing stabilized at a doubling of $CO_2$.

A tight correlation across the CMIP5 models between the sensitivity of land carbon storage to warming ($\gamma_{LT}$) and the short-term sensitivity of atmospheric $CO_2$ to tropical temperature variability ($\gamma_{IAV}$) is found. The only obvious divergence from the relationship is the MPI-ESM-LR model, which shows a unique positive correlation between anomalies in temperature and soil respiration, which seems at odds with observations. This model was therefore excluded from our linear regression. The two ESMs with an interactive nitrogen cycle (NorESM1-ME and CESM-BGC) produce the lowest values of $\gamma_{LT}$ along with unrealistically low values of $\gamma_{IAV}$, but still broadly fit the best fit emergent relationship.

Overall, a linear correlation between $\gamma_{LT}$ and $\gamma_{IAV}$ is derived from both the Historical and the 1%COU CMIP5 model ensemble, thus confirming previous results found for the $C^4$MIP ensemble [*Cox et al.*, 2013]. However, this straight line in the $\gamma_{LT}$ and $\gamma_{IAV}$ space has a different gradient in all three ensembles, owing to the different scenarios prescribed in each of these intercomparison exercises. The time scale $\tau$ in the theoretical framework for the emergent constraint is therefore most likely related to the rate of climate change, which is largely determined by the particular scenario imposed for each of the ensembles.

Constraining both ensembles with observations results long-term sensitivities, $\gamma_{LT}$, that are very similar (CMIP5: $-44 \pm 14$ GtC/K and $C^4$MIP: $-53 \pm 17$ GtC/K). It therefore seems that this emergent constraint is robust to changes in the model ensemble, to the experimental design (i.e., whether the $CO_2$ concentration is prescribed or interactive), and to the scenario prescribed.

Emergent constraints of this type, between observable aspect of variability and long-term Earth System Sensitivities, offer a very promising approach to reduce the uncertainties in climate change projections. We hope that this paper will act as some stimulus for others to search for emergent constraints among the growing ensemble of complex ESMs that are now becoming available for analysis.

**Acknowledgments**

This work was funded by the European Commission's Seventh Framework Programme, under grant agreement 282672, the "Earth system Model Bias Reduction and assessing Abrupt Climate change (EMBRACE)" project, and the DLR "Earth System Model Validation (ESMVal)" project. We acknowledge the World Climate Research Program's (WCRP) Working Group on Coupled Modeling (WGCM), which is responsible for CMIP, and we thank the climate modeling groups for producing and making available their model output. For CMIP, the U.S. Department of Energy's Program for Climate Model Diagnosis and Intercomparison provides coordinating support and led development of software infrastructure in partnership with the Global Organization for Earth System Science Portals. We thank ETH Zurich for help in accessing data from the ESGF archive. Thanks also to Chris Jones and Colin Prentice for their helpful reviews, and Eddy Robertson and Mattia Righi for constructive discussions and comments.

## References

Anav, A., P. Friedlingstein, M. Kidston, L. Bopp, P. Ciais, P. Cox, C. Jones, M. Jung, R. Myneni, and Z. Zhu (2013), Evaluating the land and ocean components of the global carbon cycle in the CMIP5 Earth System Models, *J. Clim.*, *26*, 6801–6843.

Arora, V. K., J. F. Scinocca, G. J. Boer, J. R. Christian, K. L. Denman, G. M. Flato, V. V. Kharin, W. G. Lee, and W. J. Merryfield (2011), Carbon emission limits required to satisfy future representative concentration pathways of greenhouse gases, *Geophys. Res. Lett.*, *38,* L05805, doi:10.1029/2010GL046270.

Arora, V. K., et al. (2013), Carbon-concentration and carbon-climate feedbacks in CMIP5 Earth system models, *J. Clim.*, *26*(15), 5289–5314, doi:10.1175/JCLI-D-12-00494.1.

Assmann, K. M., M. Bentsen, J. Segschneider, and C. Heinze (2010), An isopycnic ocean carbon cycle model, *Geosci. Model Dev.*, *3*(1), 143–167, doi:10.5194/gmd-3-143-2010.

Aumont, O. (2003), An ecosystem model of the global ocean including Fe, Si, P colimitations, *Global Biogeochem. Cycles*, *17*(2), 1060, doi:10.1029/2001GB001745.

Bell, T. (1980), Climate sensitivity from fluctuation dissipation: Some simple model tests, *J. Atmos. Sci.*, *37*, 1700–1707.

Booth, B. B. B., C. D. Jones, M. Collins, I. J. Totterdell, P. M. Cox, S. Sitch, C. Huntingford, R. A. Betts, G. R. Harris, and J. Lloyd (2012), High sensitivity of future global warming to land carbon cycle processes, *Environ. Res. Lett.*, *7*(2), 024002, doi:10.1088/1748-9326/7/2/024002.

Bousquet, P. (2000), Regional changes in carbon dioxide fluxes of land and oceans since 1980, *Science*, *290*(5495), 1342–1346, doi:10.1126/science.290.5495.1342.
Ciais, P., et al. (2005), Europe-wide reduction in primary productivity caused by the heat and drought in 2003, *Nature*, *437*(7058), 529–533, doi:10.1038/nature03972. [Available at http://www.ncbi.nlm.nih.gov/pubmed/16177786.] (Accessed 21 February 2014).
Clark, D. B., et al. (2011), The Joint UK Land Environment Simulator (JULES), model description. Part 2: Carbon fluxes and vegetation dynamics, *Geosci. Model Dev.*, *4*(3), 701–722.
Collins, W. J., et al. (2011), Development and evaluation of an Earth-System model – HadGEM2, *Geosci. Model Dev.*, *4*(4), 1051–1075, doi:10.5194/gmd-4-1051-2011.
Cox, P. M. (2001), Description of the "TRIFFID" Dynamic Global Vegetation Model, *Hadley Cent. Tech. Note*, *24*, 1–17.
Cox, P. M., R. A. Betts, C. D. Jones, S. A. Spall, and I. J. Totterdell (2000), Acceleration of global warming due to carbon-cycle feedbacks in a coupled climate model, *Nature*, *408*(6809), 184–187.
Cox, P. M., D. Pearson, B. B. Booth, P. Friedlingstein, C. Huntingford, C. D. Jones, and C. M. Luke (2013), Sensitivity of tropical carbon to climate change constrained by carbon dioxide variability, *Nature*, *494*(7437), 341–344, doi:10.1038/nature11882.
Denman, K. L., et al. (2007), Couplings between changes in the climate system and biogeochemistry, in *Climate Change 2007: The Physical Science Basis. Contribution of Working Group I to the Fourth Assessment Report of the Intergovernmental Panel on Climate Change*, edited by S. Solomon and D. Qin, pp. 499–587, Cambridge, U. K., and New York.
Dufresne, J.-L., et al. (2013), Climate change projections using the IPSL-CM5 Earth System Model: From CMIP3 to CMIP5, *Clim. Dyn.*, *40*(9–10), 2123–2165, doi:10.1007/s00382-012-1636-1.
Dunne, J. P., et al. (2012), GFDL's ESM2 global coupled climate–carbon Earth System Models. Part I: Physical formulation and baseline simulation characteristics, *J. Clim.*, *25*(19), 6646–6665, doi:10.1175/JCLI-D-11-00560.1.
Fasullo, J. T., and K. E. Trenberth (2012), A less cloudy future: The of subtropical subsidence in climate sensitivity, *Science*, *338*, 792–794.
Flato, G., et al. (2013), Evaluation of climate models, in *Climate Change 2013: The Physical Science Basis. Contribution of Working Group I to the Fifth Assessment Report of the Intergovernmental Panel on Climate Change*, edited by T. F. Stocker et al., 741–882, Cambridge Univ. Press, Cambridge, U. K., and New York.
Francey, R. J., M. Trolier, C. E. Allison, J. W. C. White, I. G. Enting, and P. P. Tans (1995), Changes in oceanic and terrestrial carbon uptake since 1982, *Nature*, *373*(6512), 326–330, doi:10.1038/373326a0.
Friedlingstein, P., L. Bopp, P. Ciais, J. Dufresne, L. Fairhead, P. Monfray, and J. Orr (2001), Positive feedback between future climate change and the carbon cycle climate impact on land uptake, *Geophys. Res. Lett.*, *28*(8), 1543–1546, doi:10.1029/2000GL012015.
Friedlingstein, P., J. Dufresne, P. Cox, and P. Rayner (2003), How positive is the feedback between climate change and the carbon cycle?, *Tellus B*, *55*, 692–700.
Friedlingstein, P., et al. (2006), Climate + carbon cycle feedback analysis: Results from the C4MIP model intercomparison, *J. Clim.*, *19*(14), 3337–3353, doi:10.1175/jcli3800.1.
Gent, P. R., et al. (2011), The Community Climate System Model version 4, *J. Clim.*, *24*(19), 4973–4991, doi:10.1175/2011JCLI4083.1.
Giorgetta, M. A., et al. (2013), Climate and carbon cycle changes from 1850 to 2100 in MPI-ESM simulations for the Coupled Model Intercomparison Project phase 5, *J. Adv. Model. Earth Syst.*, *5*(3), 572–597, doi:10.1002/jame.20038.
Griffies, S. M., M. J. Harrison, R. C. Pacanowski, and A. Rosati (2004), A technical guide to MOM4. GFDL ocean group Technical Report No. 5, *Princeton, NJ NOAA/Geophysical Fluid Dyn. Lab.*, 342 pp.
Hall, A., and X. Qu (2006), Using the current seasonal cycle to constrain snow albedo feedback in future climate change, *Geophys. Res. Lett.*, *33,* L03502, doi:10.1029/2005GL025127.
Huntingford, C., and P. M. Cox (2000), An analogue model to derive additional climate change scenarios from existing GCM simulations, *Clim. Dyn.*, *16*(8), 575–586.
Huntingford, C., et al. (2013), Simulated resilience of tropical rainforests to $CO_2$-induced climate change, *Nat. Geosci.*, *6*(4), 1–6, doi:10.1038/ngeo1741.
Iversen, T., et al. (2012), The Norwegian Earth System Model, NorESM1-M – Part 2: Climate response and scenario projections, *Geosci. Model Dev. Discuss.*, *5*(3), 2933–2998, doi:10.5194/gmdd-5-2933-2012.
Jones, C., and P. Cox (2005), On the significance of atmospheric $CO_2$ growth rate anomalies in 2002–2003, *Geophys. Res. Lett.*, *32*, L14816, doi:10.1029/2005GL023027.
Jupp, T. E., P. M. Cox, A. Rammig, K. Thonicke, W. Lucht, and W. Cramer (2010), Development of probability density functions for future South American rainfall, *New Phytol.*, *187*(3), 682–693.
Karpechko, A. Y., D. Maraun, and V. Eyring (2013), Improving future Antarctic total ozone projections by processing oriented multiple diagnostic ensemble regression, *J. Clim.*, *70*(12), 1–31.
Keeling, C., T. Whorf, M. Wahlen, and J. Plicht (1995), Interannual extremes in the rate of rise of atmospheric carbon dioxide since 1980, *Nature*, *375*, 666–670.
Keeling, C. D., S. C. Piper, and M. Heimann (1989), A three-dimensional model of atmospheric $CO_2$ transport based on observed winds: 4. Mean annual gradients and interannual variations, in *Aspects of Climate Variability in the Pacific and the Western Americas*, *Geophys. Monogr. Ser.*, vol. 55, pp. 305–363, AGU, Washington, D. C., doi:10.1029/GM055p0305.
Kirk-Davidoff, D. B. (2009), On the diagnosis of climate sensitivity using observations of fluctuations, *Atmos. Chem. Phys.*, *9*, 813–822.
Knorr, W. (2000), Annual and interannual $CO_2$ exchanges of the terrestrial biosphere: Process-based simulations and uncertainties, *Global Ecol. Biogeogr.*, *9*(3), 225–252, doi:10.1046/j.1365-2699.2000.00159.x.
Krinner, G. (2005), A dynamic global vegetation model for studies of the coupled atmosphere-biosphere system, *Global Biogeochem. Cycles*, *19*, GB1015, doi:10.1029/2003GB002199.
Lawrence, D., et al. (2011), Parameterization improvements and functional and structural advances in Version 4 of the Community Land Model, *J. Adv. Model. Earth Syst.*, *3*(3), M03001, doi:10.1029/2011MS000045.
Leith, C. (1975), Climate response and fluctuation dissipation, *J. Atmos. Sci.*, *32*, 2022–2026.
Le Quéré, C., et al. (2013), The global carbon budget 1959–2011, *Earth Syst. Sci. Data*, *5*(1), 165–185, doi:10.5194/essd-5-165-2013.
Nakicenovic, N., et al. (2000), *Emissions Scenarios: Summary for Policymakers*.
O'Gorman, P. A. (2012), Sensitivity of tropical precipitation extremes to climate change, *Nat. Geosci.*, *5*, 697–700.
Qu, X., and A. Hall (2013), On the persistent spread in snow-albedo feedback, *Clim. Dyn.*, *42*(1–2), 69–81, doi:10.1007/s00382-013-1774-0.
Raddatz, T. J., C. H. Reick, W. Knorr, J. Kattge, E. Roeckner, R. Schnur, K.-G. Schnitzler, P. Wetzel, and J. Jungclaus (2007), Will the tropical land biosphere dominate the climate–carbon cycle feedback during the twenty-first century?, *Clim. Dyn.*, *29*(6), 565–574, doi:10.1007/s00382-007-0247-8. [Available at http://link.springer.com/10.1007/s00382-007-0247-8.] (Accessed 2 June 2013).

Rammig, A., T. Jupp, K. Thonicke, B. Tietjen, J. Heinke, S. Ostberg, W. Lucht, W. Cramer, and P. Cox (2010), Estimating the risk of Amazonian forest dieback, *New Phytol.*, *187*(3), 694–706.

Reichstein, M., et al. (2007), Reduction of ecosystem productivity and respiration during the European summer 2003 climate anomaly: A joint flux tower, remote sensing and modelling analysis, *Global Change Biol.*, *13*(3), 634–651, doi:10.1111/j.1365-2486.2006.01224.x. [Available at http://doi.wiley.com/10.1111/j.1365-2486.2006.01224.x.] (Accessed 26 February 2014).

Sato, H., A. Itoh, and T. Kohyama (2007), SEIB-DGVM: A new Dynamic Global Vegetation Model using a spatially explicit individual-based approach, *Ecol. Modell.*, *200*(3–4), 279–307 ST – SEIB–DGVM: A new Dynamic Global Vege.

Schneising, O., M. Reuter, M. Buchwitz, J. Heymann, H. Bovensmann, and J. P. Burrows (2014), Terrestrial carbon sink observed from space: Variation of growth rates and seasonal cycle amplitudes in response to interannual surface temperature variability, *Atmos. Chem. Phys.*, *14*(1), 133–141, doi:10.5194/acp-14-133-2014.

Smith, T. M., R. W. Reynolds, T. C. Peterson, and J. Lawrimore (2008), Improvements to NOAA's historical merged land & ocean surface temperature analysis, *J. Clim.*, *21*(10), 2283–2296.

Taylor, K. E., R. J. Stouffer, and G. Meehl (2012), An overview of CMIP5 and the experiment design, *Bull. Am. Meteorol. Soc.*, *93*(4), 485–498, doi:10.1175/BAMS-D-11-00094.1.

Thornton, P. E., J.-F. Lamarque, N. A. Rosenbloom, and N. M. Mahowald (2007), Influence of carbon-nitrogen cycle coupling on land model response to $CO_2$ fertilization and climate variability, *Global Biogeochem. Cycles*, *21*, GB4018, doi:10.1029/2006GB002868.

Thornton, P. E., S. C. Doney, K. Lindsay, J. K. Moore, N. Mahowald, J. T. Randerson, I. Fung, J.-F. Lamarque, J. J. Feddema, and Y.-H. Lee (2009), Carbon-nitrogen interactions regulate climate-carbon cycle feedbacks: Results from an atmosphere-ocean general circulation model, *Biogeosciences*, *6*(10), 2099–2120, doi:10.5194/bg-6-2099-2009.

Verseghy, D. L., N. A. McFarlane, and M. Lazare (1993), Class - A Canadian land surface scheme for GCMS, II. Vegetation model and coupled runs, *Int. J. Climatol.*, *13*(4), 347–370, doi:10.1002/joc.3370130402.

Watanabe, S., et al. (2011), MIROC-ESM: Model description and basic results of CMIP5-20c3m experiments, *Geosci. Model Dev. Discuss.*, *4*(2), 1063–1128, doi:10.5194/gmdd-4-1063-2011. [Available at http://www.geosci-model-dev-discuss.net/4/1063/2011/.] (Accessed 29 April 2013).

Zaehle, S., P. Friedlingstein, and A. D. Friend (2010), Terrestrial nitrogen feedbacks may accelerate future climate change, *Geophys. Res. Lett.*, *37*, L01401, doi:10.1029/2009GL041345.

Zahariev, K., J. R. Christian, and K. L. Denman (2008), Preindustrial, historical, and fertilization simulations using a global ocean carbon model with new parameterizations of iron limitation, calcification, and N2 fixation, *Prog. Oceanogr.*, *77*(1), 56–82, doi:10.1016/j.pocean.2008.01.007.